

Cite this: *New J. Chem.*, 2012, **36**, 674–684

www.rsc.org/njc

PAPER

Probing the surface polarity of inorganic oxides using merocyanine-type dyes derived from barbituric acid†

Susan Seifert,^a Andreas Seifert,^a Gunther Brunklaus,^b Katja Hofmann,^a Tobias Rüffer,^c Heinrich Lang^c and Stefan Spange^{*a}

Received (in Montpellier, France) 28th September 2011, Accepted 23rd November 2011

DOI: 10.1039/c2nj20835k

The solid state complexes, solvatochromic and acidochromic behaviour of four merocyanine-type dyes derived from barbituric and thiobarbituric acid and their use as solvatochromic probe molecules for coloured surfaces are described. The dyes were obtained by condensation reaction of barbituric, *N*-methylbarbituric, *N,N'*-dimethylbarbituric and thiobarbituric acid with 4-*N*, *N*-dimethylaminocinnamaldehyde. The dyes were characterised by means of liquid and solid state NMR techniques (¹H MAS NMR, ¹H–¹H DQ MAS NMR, ¹³C CPMAS NMR), single-crystal X-ray analysis, UV/vis and IR measurements. The solvatochromism has been investigated in 43 solvents and interpreted in terms of Kamlet–Taft parameters α , β , and π^* . Altogether, the solvatochromic properties of these four dyes were determined mainly by the hydrogen bond donating (HBD) ability and the polarisability/dipolarity of a solvent. The interactions of the dyes with oxidic and metal surfaces were studied. Their perichromic behaviour was compared with that of established solvatochromic dyes for the determination of α , β , and π^* , namely dicyano-bis-(1,10-phenanthroline)-iron(II)-complex (**1**), 3-(4-amino-3-methylphenyl)-7-phenyl-benzo-[1,2-*b*:4,5-*b'*]-difuran-2,6-dione (**2**) and 4-*tert*-butyl-2-(dicyanomethylene)-5-[4-(diethylamino)benzylidene]- Δ^3 -thiazoline (**3**). The barbituric acid dyes were used to probe the surface polarity of coloured oxides like tungsten(VI) oxide and iron(III) oxide. The interactions between the dyes and metals like zinc and aluminium were also investigated.

Introduction

The surface polarity of inorganic oxides constitutes an important factor for many practical applications, and potentially allows for a deeper understanding of the catalytic activity of inorganic oxides in heterogeneous catalysis, interactions between oxidic surfaces and adsorbed polymer films or the integration of inorganic fillers into organic matrices, respectively.^{1–13} However, the term *polarity* itself has, until now, not been precisely defined and cannot be merely quantified by means of individual physical constants such as the relative permittivity or dipole moments.¹⁴ In the past, several empirical methods have been introduced to determine the polarity of solvents *via* solvatochromic probe dyes,

including rather simplistic single-parameter approaches of *e.g.* Kosower's Z-scale,¹⁵ Gutmann's acceptor (AN) and donor number (DN),¹⁶ or Dimroth–Reichardt's E_T30 scale¹⁷ as well as multi-parameter approaches of *e.g.* Kamlet–Taft's α , β , and π^* scale,¹⁸ or Catalán's SA, SB, SP and SdP scale.¹⁹ Notably, such measurements are based on monitoring solvent-dependent shifts of the UV/vis absorption band of a probe dye resulting from both rather specific (*e.g.* hydrogen bond donating (HBD) or hydrogen bond accepting (HBA)) and non-specific interactions (including dipole–dipole, dipole–induced dipole, or even dispersion forces), while interactions that chemically alter the probe dye are disregarded.²⁰ The Kamlet–Taft and Catalán approaches have been successfully applied to separate these influences,^{18,19} but based on practical considerations the simplified Kamlet–Taft equation was evaluated and used in this work, given as eqn (1),¹⁸

$$\tilde{\nu}_{\max} = \tilde{\nu}_{\max,0} + a\alpha + b\beta + s\pi^* \quad (1)$$

where $\tilde{\nu}_{\max,0}$ denotes the value of a solvent reference system such as the nonpolar medium cyclohexane. The parameter α describes the HBD ability, β the HBA ability, and π^* represents the dipolarity/polarisability, respectively. In addition, a , b , and s are solvent-independent coefficients reflecting contributions of solvent effects to the UV/vis absorption shift $\tilde{\nu}_{\max}$.

^a Department of Polymer Chemistry, Chemnitz Technical University, Strasse der Nationen 62, 09107 Chemnitz, Germany.

E-mail: stefan.spange@chemie.tu-chemnitz.de;

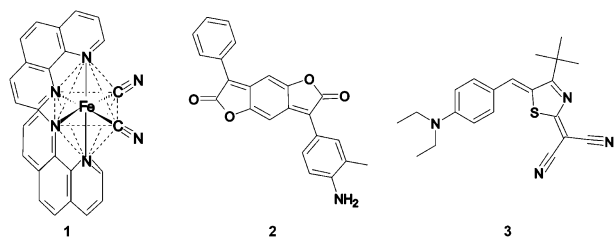
Fax: +49 (0) 37 1 53 12 12 39; Tel: +49 (0) 37 1 53 12 12 30

^b Department of Physical Chemistry, University of Muenster,

Corrensstrasse 28/30, 48149 Muenster, Germany

^c Department of Inorganic Chemistry, Chemnitz Technical University, Strasse der Nationen 62, 09107 Chemnitz, Germany

† Electronic supplementary information (ESI) available: CIF file of compound **4**; spectral data and spectra, which are not shown in the manuscript as well as solvent parameters known from the literature. CCDC reference number 822677. For ESI and crystallographic data in CIF or other electronic format see DOI: 10.1039/c2nj20835k



Scheme 1 Solvatochromic (perichromic) dyes **1–3** suitable for measurement of surface polarities.

The application of solvatochromic probes for the determination of solvent and surface polarity is rather advantageous since a quite small concentration of the corresponding dye is required while the method is rather sensitive and reproducible. Note that, to utilize solvatochromic probes on surfaces at the microscopic level, the term perichromism has been suggested.^{17,21}

Indeed, several perichromic probes were used to characterise the surface polarity parameters α , β , and π^* , respectively, of “white” powders, including *e.g.* cellulose, SiO₂, Al₂O₃, or aluminosilicates *via* dyes **1–3** shown in Scheme 1.^{7,22,23}

In particular, the dicyano-bis-(1,10-phenanthroline)-iron(II) complex **1** is a well-established probe molecule for the determination of both the acceptor number AN and HBD ability α of metal ions, solvents, binary mixtures of solvents, polymers, particle surfaces, polymer-modified particles and ionic liquids.^{7d–f,i,m,24–33} In contrast, the HBA ability β of solvents, polymers, ionic liquids and surfaces can be quantified with 3-(4-amino-3-methylphenyl)-7-phenyl-benzo-[1,2-*b*:4,5-*b'*]-difuran-2,6-dione (**2**) while π^* can be identified using 4-*tert*-butyl-2-(dicyano-methylene)-5-[4-(diethylamino)benzylidene]- Δ^3 -thiazoline (**3**).^{7d,e,i,34–37} Based on eqn (2)–(4), α , β , or π^* can be individually derived from the UV/vis absorption maxima of the perichromic probe dyes **1–3**.^{7b,34a}

$$\alpha = -7.49 + 0.46 \tilde{\nu}_{\max}(\mathbf{1})[10^{-3} \text{ cm}^{-1}]^{7b} \quad (2)$$

$$\beta = 3.84 - 0.20 \tilde{\nu}_{\max}(\mathbf{2})[10^{-3} \text{ cm}^{-1}]^{7b} \quad (3)$$

$$\pi^* = 9.475 - 0.54 \tilde{\nu}_{\max}(\mathbf{3})[10^{-3} \text{ cm}^{-1}]^{34a} \quad (4)$$

However, experiences in the field of perichromism of strongly coloured metal oxides such as iron(III) oxide or tungsten(VI) oxide and industrially important metal powders, including aluminium, zinc, iron, steel or copper, are up to now rather limited. Notably, such perichromic probe dyes have to fulfill several threshold criteria: while the wavelength of the UV/vis absorption maxima of the considered dye(s) should be larger than 570 nm, successful and reversible adsorption at either the metal or metal oxide surface must be associated with a significant measurable UV/vis shift, which can be difficult to achieve. Though dyes **1** and **3** have UV/vis absorption maxima in the range of 570–640 nm, respectively,^{25a,34d} their adsorption onto metal surfaces did not yield detectable UV/vis spectra,³⁸ therefore rendering a search for alternative dyes necessary.

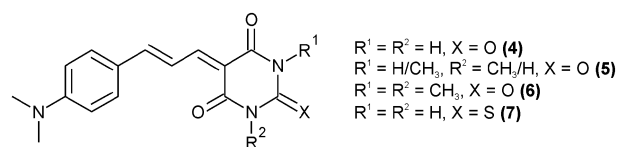
It is known that both barbituric and thiobarbituric acid derivatives interact with ions of heavy metals,^{39–42} while barbituric acid and *N,N'*-dimethylbarbituric acid derivatives obtained from *N,N*-dimethylaminobenzaldehyde or 4,4'-bis(dimethylamino)-benzophenone exhibit solvatochromic behaviour.^{43–45} Their UV/vis absorption maxima are in the range of 450–470 nm and

474–586 nm, respectively. They show rather broad absorption bands in HBD media. This effect was first reported by Rezende *et al.* and attributed to protonation of carbonyl units comprising the barbituric acid moiety, rendering these dyes less suitable for application as perichromic probes of Lewis acid metal oxide surfaces. Though barbituric and thiobarbituric acid dyes obtained from retinal, without the presence of strong electron donor substituents, may exhibit enlarged conjugated π -systems, no indication of successful proton transfer in HBD media was found.⁴⁵ However, the corresponding absorption maxima were identified in the range of 468–526 nm, thus excluding these dyes for analysis of strongly coloured surfaces.⁴⁵

A rather better perichromic dye may be designed according to a balance between both the length of the π -system and the electron donor system thereby yielding UV/vis absorption maxima larger than 570 nm, and it should not be protonated in HBD media. In the present work, (thio)barbituric acid derivatives carrying a *N,N*-dimethylamino group as electron donor substituent and two conjugated exocyclic double bonds (*cf.* Scheme 2) were explored. In addition, different substituents were attached to the respective (thio)barbiturate moiety to systematically vary both the electron-demanding effects and interactions with the surrounding(s) of the dye.

In particular, such dyes are readily accessible *via* Knoevenagel condensation of corresponding (thio)barbituric acid derivatives with 4-*N,N*-dimethylaminocinnamaldehyde, and the preparation of compounds **4**, **6**, and **7** has been previously reported.^{39,46–49} Note that dyes **4**, **6**, and **7** have found interest as nonlinear optic materials,⁵⁰ as methionine aminopeptidase-1 inhibitors⁴⁹ and laser dyes.⁵¹ Further, interactions of heavy metal ions with compound **7**³⁹ including its application as photoconductor for electrophotography^{52–54} or dye in hair tinting lotions were described, while comprehensive structural data (*e.g.* single-crystal X-ray analysis) as well as investigations concerning their perichromic and acido-chromic behaviour are rather limited to date.

In the current contribution, the perichromic and acidochromic behaviour of dyes **4–7** was investigated to potentially establish the compounds for reproducible determination of the Kamlet–Taft (polarity) parameters of coloured oxidic and metallic materials. Since metal oxidic surfaces may also bear strong acidic and basic groups, non-solvatochromic interactions like acid–base reactions were also considered. Notably, dyes **4–7** were independently adsorbed onto different “white” oxidic surfaces to probe the perichromic behaviour in comparison to the rather well-established dyes **1–3**. Since occurrence of self-aggregation or polymorphism of (thio)barbituric acid derivatives is well known,⁵⁵ a detailed structural characterisation of solid dyes **4–7** is rather important. Insights into molecular arrangements of the corresponding dyes were obtained from both single-crystal X-ray analysis and multi-nuclear solid-state NMR spectroscopy including 2D homonuclear dipolar double quantum (DQ) NMR, which



Scheme 2 (Thio)barbituric acid derivatives **4–7** studied in this work.

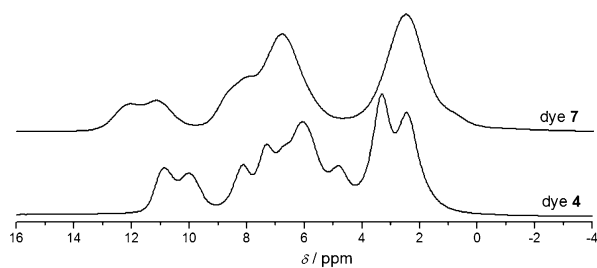


Fig. 4 ^1H MAS NMR spectra of **4** and **7**, acquired at 700.2 MHz and 50 kHz MAS.

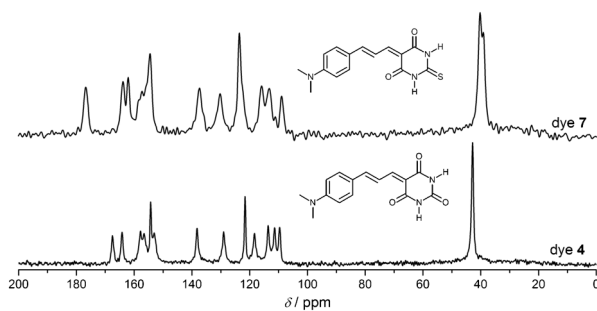


Fig. 5 $^{13}\text{C}\{-^1\text{H}\}$ -CPMAS NMR spectra of **4** and **7** acquired at 176.1 MHz and 40 kHz MAS while applying a contact time of 3 ms.

Nevertheless, the possible occurrence of bond angles even closer to 180° may also contribute to increased ^1H chemical shifts of the NH protons and cannot be excluded. Notably, unlike in all other dyes, observable $^{13}\text{C}\{-^1\text{H}\}$ -CPMAS NMR signals (Fig. 5) of the methyl groups of the aniline ring are *isochronic* in the case of compound **4**, even though hydrogen bonding of methyl groups to the oxygen atoms of the barbituric acid moiety can be found in the single-crystal structure solution of **4**.

$^1\text{H}\{-^1\text{H}\}$ double-quantum (DQ) MAS NMR is in general a highly useful and selective approach to identify close contacts or spatial proximities of structural moieties and thus can be used to reveal changes of local hydrogen-bonding environments. In such a two-dimensional experiment, double-quantum coherences (DQC) due to *pairs* of dipolar coupled protons are correlated with single-quantum coherences resulting in characteristic correlation peaks. Double-quantum coherences between so-called *like* spins appear as a single correlation peak on the diagonal (“auto-peak”) while a pair of cross-peaks that are symmetrically arranged on either side of the diagonal reflect couplings among *unlike* spins. DQ peaks appear at the sum frequency of the two coupled spins and therefore often allow for an increased spectral resolution. Strong signal intensities at short DQ excitation times of 1–2 rotor periods (20–40 μs) identify protons in close spatial proximity while weak DQ signals typically reflect long-distance contacts.⁶³ Indeed, two strong auto-correlation peaks at 21.6 ppm (DQ: 10.8 + 10.8 ppm) and 19.8 ppm (DQ: 9.9 + 9.9 ppm), respectively, in the $^1\text{H}\{-^1\text{H}\}$ DQ MAS NMR spectrum of **4** (Fig. 6) are in excellent agreement with the self-complementary aggregation of the asymmetric unit moiety with two neighbouring molecules, stabilized by $\text{HN}\cdots\text{O}$ hydrogen-bonding. In addition, the rather strong cross-peaks at 13.3 ppm (DQ: 10.9 + 2.4 ppm) and 13.2 ppm (DQ: 9.9 + 3.3 ppm) reflect the close spatial proximity of the NH protons to

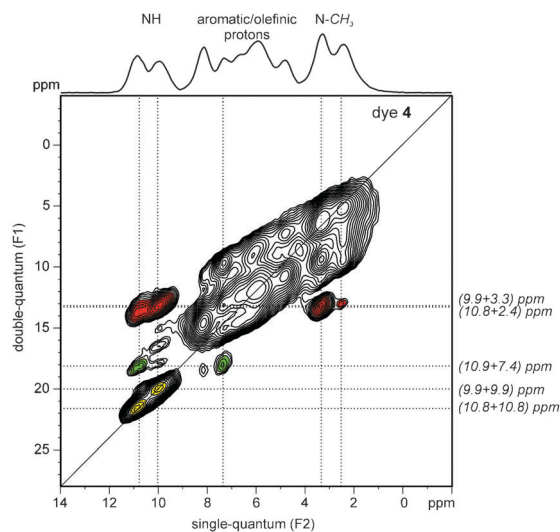


Fig. 6 $^1\text{H}\{-^1\text{H}\}$ 2D DQ MAS NMR spectrum of **4** at 700.2 MHz and 50 kHz MAS, acquired under the following experimental conditions: $162t_1$ increments at steps of 20 μs , relaxation delay 32 s, 16 transients per increment, and 40 μs DQ excitation time. The F2 projection is shown on the top.

the methyl groups. Based on the fact that the NH proton at 10.9 ppm has a reasonably strong cross-peak at 18.2 ppm (DQ: 10.9 + 7.4 ppm), it is assigned to the crystallographic H2N site, which at least within a threshold distance of about 4.5 Å has more contacts to olefinic protons (see ESI†) than the H3N site (attributed to the peak at 9.9 ppm).

Similar to the case of **4**, the $^1\text{H}\{-^1\text{H}\}$ DQ MAS NMR spectrum of **7** exhibits two strong auto-peaks at 24.2 ppm (DQ: 12.1 + 12.1 ppm) and 22.2 ppm (DQ: 11.1 + 11.1 ppm), respectively, which can be attributed to the two NH protons. However, only one of the two NH protons has a strong cross-peak with the methyl group (DQ: 12.1 + 2.4 ppm), while an anticipated peak at 13.5 ppm (DQ: 11.1 + 2.4 ppm) is absent. In addition, the comparatively stronger cross-peaks with aromatic or olefinic protons at either 20.6 ppm (DQ: 12.1 + 8.5 ppm), 18.8 ppm (DQ: 12.1 + 6.7 ppm) or 17.8 ppm (DQ: 11.1 + 6.7 ppm) suggest a different spatial packing of the (thio)barbiturate moieties in compound **7** than found in dye **4** (Fig. 7).

In the case of **5**, the auto-peak of the NH proton at 22.6 ppm (DQ: 11.3 + 11.3 ppm) in the $^1\text{H}\{-^1\text{H}\}$ DQ MAS NMR spectrum clearly indicates the presence of hydrogen bonded “dimers” in the solid compound (consistent with dyes **4** and **7**), while a similarly strong cross-peak at 13.9 ppm (DQ: 11.3 + 2.6 ppm) reflects the contact of the NH proton with the methyl group. Combined with the $^{13}\text{C}\{-^1\text{H}\}$ -CPMAS NMR spectrum, this allows us to propose the tentative structure of solid dye **5** displayed in Fig. 8.

Due to the absence of NH protons in compound **6**, the formation of “dimers” based on strong directional hydrogen-bonding is not possible. However, though weakly stabilized aggregates are in principle feasible, the measured $^1\text{H}\{-^1\text{H}\}$ DQ MAS NMR spectrum of **6** is not sufficiently conclusive to propose a resulting structure (ESI†). Nevertheless it should be noted that the $^{13}\text{C}\{-^1\text{H}\}$ -CPMAS NMR spectrum of **6** is somewhat similar to that of dye **5**.

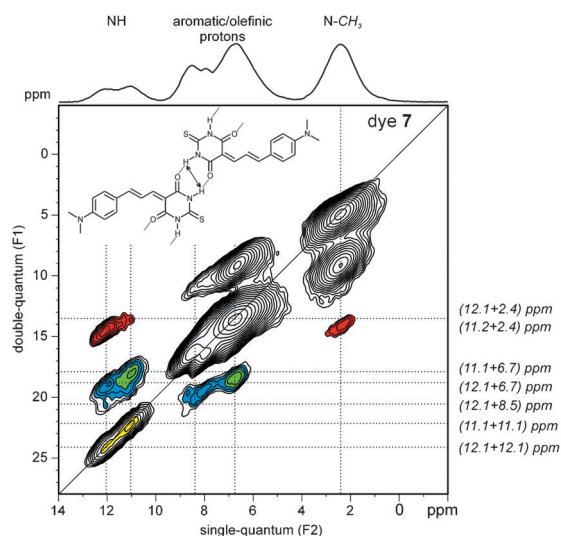


Fig. 7 ^1H - ^1H 2D DQ MAS NMR spectrum of **7** at 700.2 MHz and 50 kHz MAS, acquired under the following experimental conditions: $162t_1$ increments at steps of 20 μs , relaxation delay 32 s, 16 transients per increment, and 40 μs DQ excitation time. The F2 projection is shown on the top.

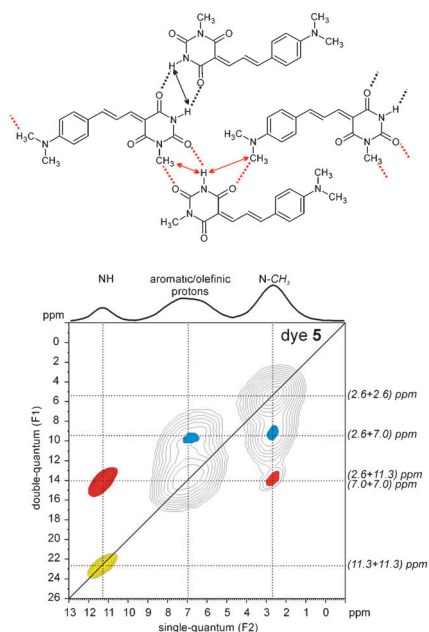


Fig. 8 ^1H - ^1H 2D DQ MAS NMR spectrum of **5** at 700 MHz and 29762 Hz MAS, acquired under the following experimental conditions: $96t_1$ increments at steps of 33.6 μs , relaxation delay 7 s, 32 transients per increment. The F2 projection is shown on the top.

Solvatochromism

The solvatochromic properties of dyes **4–7** were studied in 43 HBD and HBA solvents (see Table 1 and ESI†).

The observed UV/vis absorption bands were found in the range of 473–587 nm (dyes **4–6**) and 517–613 nm (dye **7**), respectively, irrespective of the dye concentration, exhibiting a moderate to large solvatochromic UV/vis shift range and high extinction coefficients in different organic solvents (Tables 1 and 2).

Table 1 UV/vis absorption maxima of compounds **4–7** in selected solvents, the extent of the solvatochromic shift, as well as the solvent polarity parameter sets of Kamlet–Taft⁶⁴

Solvents	$\tilde{\nu}_{\text{max}}(\text{dye})/10^3 \text{ cm}^{-1}$				α^{64}	β^{64}	π^{*64}
	4	5	6	7			
Acetone	19.59	19.51	19.47	18.03	0.08	0.43	0.71
Dioxane	20.20	20.12	20.12	18.59	0.00	0.37	0.55
1,2-Ethanediol	17.86	17.92	17.98	16.79	0.90	0.52	0.92
HFIP ^{a,b}	17.08	17.05	17.09	16.31	1.96	0.00	0.65
Toluene	19.42	19.46	19.66	17.97	0.00	0.11	0.54
Triethylamine ^c	21.14	20.79	20.12	19.34	0.00	0.71	0.14
$\Delta\lambda/\text{nm}$	113	106	88	96			
$\Delta\tilde{\nu}/\text{cm}^{-1}$	4060	3740	3030	3030			

^a 1,1,1,3,3,3-Hexafluoroisopropanol. ^b Solvent with the highest bathochromic shift. ^c Solvent with the highest hypsochromic shift.

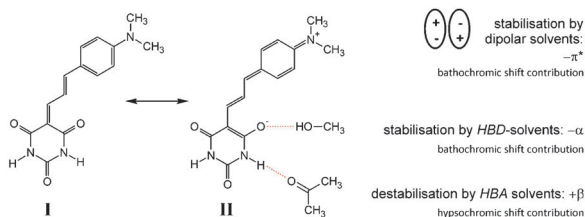
Table 2 Extinction coefficient of compound **4–7**

Compound	$\epsilon/\text{L mol}^{-1} \text{ cm}^{-1}$	
	Dichloromethane	Acetonitrile
4	61 000	55 000
5	62 000	55 000
6	55 000	55 000
7	57 000	43 000

The individual influences of either specific and/or non-specific solvent–dye interactions of both HBA and HBD solvents on the position of the UV/vis absorption band have been evaluated by means of multiple regression analysis using the solvent polarity parameter sets of Kamlet–Taft (see ESI†). Furthermore, non-HBD and HBD solvents were also considered separately for discussion.

Reasonable correlations can only be obtained, excluding several solvents (such as aniline, piperidine, trichloroacetic acid and trifluoroacetic acid) from correlation analysis. Notably, non-solvatochromic reactions including protonation (trifluoroacetic acid or trichloroacetic acid) or degradation reactions (piperidine) were observed. When all tested solvents or solely the non-HBD solvents are considered, the (thio)barbituric acid derivatives **4**, **5**, and **7** with their NH-acidic pyrimidone nitrogen group reveal solvatochromic behaviour as a function of the three solvent parameters, α , β , and π^* , respectively. In contrast, for explanation of the solvatochromic behaviour of the dimethyl-functionalised barbituric derivative **6**, the influence of the parameter β can be neglected. Furthermore, the thiobarbituric acid derivative **7** exhibited consistently lower transition energies compared to the barbituric acid derivatives **4–6** when measured in the same solvent. The collective results are in good agreement with the solvatochromic behaviour of similar barbituric acid merocyanine-type dyes.^{43,45}

Non-specific interactions. Non-specific interactions are expressed with the Kamlet–Taft's π^* parameter. As expected for this class of barbituric acid merocyanine-type dyes,^{43,45} positive solvatochromism (bathochromic shift of the UV/vis absorption band with increasing dipolarity/polarisability π^* of the solvent as indicated by a large negative s term) with regard to this parameter is observed. Therefore, the electronically excited state exhibits a higher dipole moment and is stabilised by solvents with rather high polarisability/dipolarity. A charge-transfer from



Scheme 3 Schematic representation of two possible resonance structures of dye **4** and explanation of the influences of specific and non-specific solvent–dye interactions on the solvatochromic behaviour.

the *N,N*-dimethylamino group (donor) to the oxygen atoms in positions 4 and 6 of the (thio)-barbituric acid moiety (acceptor) leads to a zwitterionic resonance structure (Scheme 3). In the electronically excited state this zwitterionic resonance structure II dominates the neutral resonance structure I, whereas in the ground state the reverse case is found.

Specific interactions. Specific dye–solvent interactions are expressed by both, the HBD ability (acidity) α and HBA ability (basicity) β . Interactions of HBD solvents with a (thio)barbiturate carbonyl moiety lead to a decrease of their electron density and an increase of the push–pull character of the chromophores, thus resulting in a bathochromic UV/vis shift contribution. Indeed, HBA solvents are able to interact with the NH-acidic pyrimidone nitrogen groups of dyes **4**, **5**, and **7**, respectively, which increases the electron density of the (thio)barbituric acid moiety and therefore, the push–pull character of the dyes decreases. These effects destabilise the electronically excited state yielding a hypsochromic UV/vis shift contribution.

Thus, with increasing HBD strength and polarisability/dipolarity of the considered solvent, the observable UV/vis absorption band shifted bathochromically (Fig. 9).

The physicochemical results of the correlation square analysis are different when only HBD solvents are considered (Table 3, HBD solvents). Using the Kamlet–Taft parameters the solvatochromic behaviour seems to be only dependent on β and π^* . According to the work of Rezende and co-workers,⁴³ it is likely that the formation of strong hydrogen bonds between the (thio)barbituric acid moiety of the dyes in more

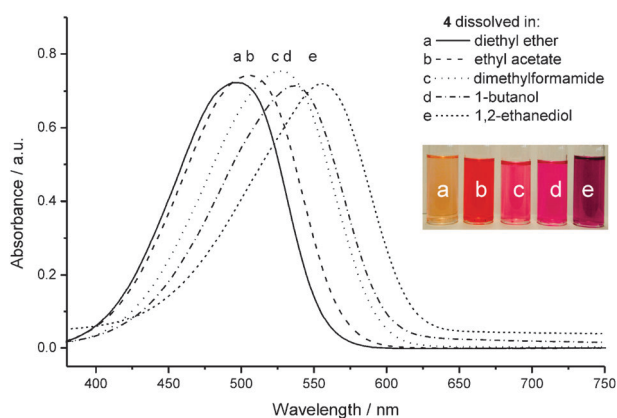


Fig. 9 UV/vis absorption spectra and photo of **4** dissolved in five different solvents.

Table 3 Values of solvent-independent correlation coefficients a , b , and s for the Kamlet–Taft equation: $\tilde{\nu}_{\max} = \tilde{\nu}_{\max,0} + a\alpha + b\beta + s\pi^*$ (1), including the wavenumber of the reference system ($\tilde{\nu}_{\max,0}$), the correlation coefficient (r), the standard derivation (sd), and the number of solvents (n) of **4–7**. If not mentioned the significance f was below 0.0001

Kamlet–Taft solvent polarity parameter set								
HBD and HBA solvents								
Dye	$\tilde{\nu}_{\max,0}$	a	b	s	r	sd	n	Eqn
4	20.22	−1.17	0.89	−1.94	0.88	0.41	39	5a
5	20.35	−1.12	0.46	−1.87	0.89	0.34	40	5b
6	20.57	−1.10		−1.82	0.92	0.28	39	5c
7	18.82	−0.80	0.66	−1.81	0.90	0.28	38	5d
Non-HBD solvents								
4	20.38	−0.61	1.64	−2.51	0.94	0.27	25	5e
5	20.48	−0.63	0.93	−2.27	0.91	0.26	26	5f
6	20.78	−0.90		−2.09	0.89	0.26	26	5g
7	18.90	−0.59	1.07	−2.10	0.95	0.19	25	5h
HBD solvents								
4	17.74		1.73	−0.72	0.93	0.25	14	5i
5	17.68		1.65	−0.54	0.92	0.26	14	5k
6^a	17.69		1.45	−0.36	0.86	0.29	14	5l
7^a	17.00		1.24	−0.86	0.93	0.20	13	5m

^a $f = 0.0004$ [eqn (5l)], $f = 0.0001$ [eqn (5m)].

Brønsted acidic solvents takes place, leading to a significant change in the push–pull character of the dyes.

Acidochromism

Interactions with acids. In strong acids such as trifluoroacetic acid (TFA) ($pK_a = 0.26$), trichloroacetic acid ($pK_a = 0.08$), with HCl ($pK_a = -7$), or when adsorbed onto acidic surfaces (e.g., aluminosilicate Siral 30), UV/vis absorption bands in the range of 360–370 nm (dyes **4–6**) and at 392 nm (dye **7**) are observed (Fig. 10).

The appearance of UV/vis absorption bands at 360–370 nm (dyes **4–6**) and at 392 nm (dye **7**), respectively, is reversible with addition of NaOH and isosbestic points at 424 nm (dyes **4–6**) and at 453 nm (dye **7**) were observed. Therefore, an acid–base reaction in conjunction with the loss of the push–pull character of the compounds takes place. Rezende and co-workers⁴³ already reported on the interactions of acidic media with a compound

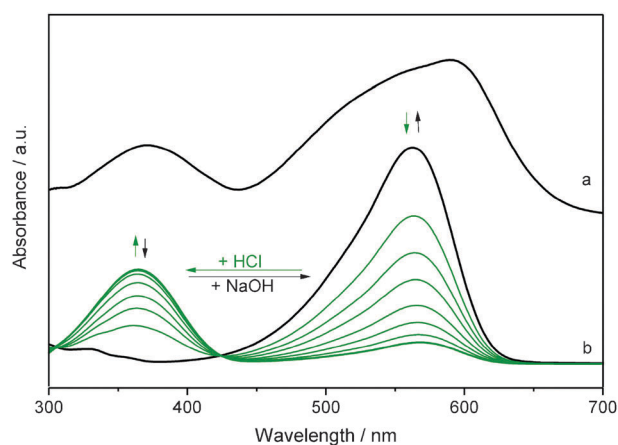


Fig. 10 Acidochromic behaviour of dye **4** adsorbed onto aluminosilicate Siral 30 (a) or dissolved in EtOH/H₂O (4/3) with HCl addition (b).

Table 4 pK_a values of dyes 4–7 determined in EtOH:H₂O (ratio 4:3/vol/vol)

Dye	R ¹	R ²	X	pK_a
4	H	H	O	0.54
5	H	CH ₃	O	0.60
6	CH ₃	CH ₃	O	0.74
7	H	H	S	0.39

obtained by condensation of *N,N'*-dimethylbarbituric acid and *N,N*-dimethylaminobenzaldehyde. Their semiempirical calculations indicated that a protonation occurs preferentially at the oxygen atoms of the barbituric acid moiety and not at the nitrogen atom of the *N,N*-dimethylamino group.⁴³ The pK_a values of dyes 4–7 concerning this protonation were determined by a UV/vis titration in an ethanol:water mixture (4:3 vol/vol) (Table 4).

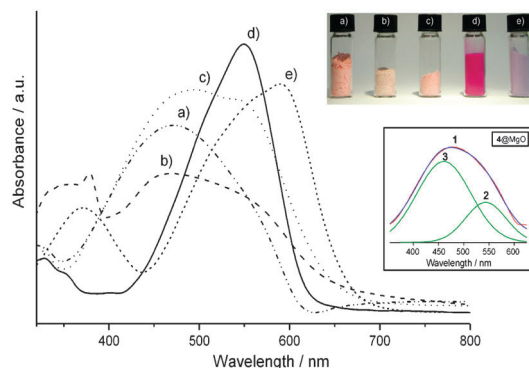
A clear trend is observed: the higher the degree of methyl-substitution of the barbituric acid moiety, the higher is the pK_a value of the dyes caused by the +I effect of the substituted methyl group(s). The thiobarbituric acid derivative has the lowest pK_a value. This can also be observed when the dyes were adsorbed onto acidic surfaces. In contrast to dye 7, protonations of dyes 4 and 6 are observed when adsorbed onto aluminosilicate Siral 30 (Fig. 10).

Interactions with bases. Interactions of 4–7 with several bases were investigated. The NH proton bearing (thio)barbituric acid dyes 4, 5, and 7 shows a different behaviour depending on the base. These are solvatochromic effects (pyridine, piperidine), deprotonation of the (thio)barbituric acid moiety (tetra-*n*-butyl ammonium fluoride [TBAF], NaOH) as well as degradation reactions (piperidine, TBAF, NaOH). The dyes 4, 5, and 7 are much more stable in basic media compared to 6. Thus, for the dimethyl-functionalised barbituric acid 6 only degradation reactions were observed using piperidine, TBAF, and NaOH, respectively. The different behaviour between the NH-bearing and the dimethyl-functionalised (thio)barbituric acid dyes and bases is exemplified by the use of TBAF in the ESI.[†]

Interactions with oxidic and metal surfaces

Interactions with oxidic surfaces. A variety of interactions between different surface centres and 4–7 can take place. Thus, UV/vis absorption spectra with a complex shape were often obtained. Representative UV/vis absorption spectra of 4 adsorbed onto five oxide surfaces are shown in Fig. 11.

Obviously, simple determination of the global UV/vis absorption maxima from the UV/vis absorption spectra is not adequate to characterize perichromic interactions in those cases. Rather, in order to identify the UV/vis absorption band attributable to perichromic effects, the UV/vis absorption spectra of dyes 4–7 were fitted with several Gaussian functions. An exemplary result is presented in Fig. 11 for 4 adsorbed onto magnesium oxide. The red curve is the original UV/vis absorption spectrum, which could be reasonably deconvoluted with two Gaussian curves (green). The resulting blue curve is nearly congruent with the original UV/vis absorption spectrum. A clear difference between the global UV/vis absorption maximum (1) at 473 nm and the isolated longest wavelength UV/vis absorption band (2) at 543 nm is

**Fig. 11** UV/vis absorption spectra of 4 adsorbed onto five different surfaces [(a) MgO, (b) ZnO, (c) CaCO₃, (d) silica gel 60, (e) aluminosilicate (see the photo)]. Inset: UV/vis absorption spectrum of 4 adsorbed onto magnesium oxide and multipeak fitting.

recognisable. The UV/vis absorption band (3) is assumed to correspond to the interaction of the dimethylamino group of molecules interacting with a positive charge, *i.e.* Mg²⁺ or Zn²⁺.

To evaluate the obtained values of the longest wavelength UV/vis absorption band of dyes 4–7 adsorbed onto different surfaces as shown in Table 5, reference polarity parameters α , β , π^* of these surfaces were required.

Therefore, the Kamlet–Taft surface polarity parameters (α , β , π^*) of these surfaces were determined by means of well-established probes 1–3 and eqn (2)–(4) (Table 6).

Inserting the reference polarity parameters α , β , and π^* of solvents⁶⁴ and surfaces (Table 6; Table S4 in the ESI[†]) in eqn (5a) (from Table 3: result of the multiple regression analysis of dye 4) leads to a theoretical value for UV/vis absorption maxima of dye 4 dissolved in different solvents/adsorbed onto oxidic surfaces. Compared to the measured UV/vis wavenumbers of 4, only small differences are identified (Fig. 12). For compounds 5–7, analogous relationships were obtained (see ESI[†]), thus rendering dyes 4–7 a viable addition to the established perichromic probe dyes 1–3, if one or two surface polarity parameters cannot be determined by probe dyes 1–3.

Table 5 Longest wavelength UV/vis absorption band of 4–7 adsorbed onto oxidic surfaces

Sample	$\tilde{\nu}_{\max,4}/10^3 \text{ cm}^{-1}$	$\tilde{\nu}_{\max,5}/10^3 \text{ cm}^{-1}$	$\tilde{\nu}_{\max,6}/10^3 \text{ cm}^{-1}$	$\tilde{\nu}_{\max,7}/10^3 \text{ cm}^{-1}$
Silica gel 60	17.61	17.70	18.08	16.92
Siral 1.5	17.42	17.42	17.79	16.37
Siral 15	17.30	17.42	17.21	16.31
Siral 30	16.98	17.04	17.36	16.13
Siral 60	16.84	16.92	17.39	15.95
Siral 80	16.84	16.84	17.27	15.95
MgO	18.40 ^a	18.25 ^a	18.44	20.23
CaCO ₃	18.13 ^a	17.71 ^a	17.86 ^a	16.55
ZnO	17.71 ^a	18.19 ^a	17.71 ^a	16.73 ^a
TiO ₂ (anatase)	17.09 ^a	17.40 ^a	18.15 ^a	16.90 ^a
TiO ₂ (rutile)	17.74 ^a	18.04 ^a	17.75 ^a	16.81 ^a
Al ₂ O ₃	17.57 ^a	17.47 ^a	18.02	16.44 ^a
WO ₃	16.92 ^a	17.15 ^a	17.22 ^a	16.05 ^a
Fe ₂ O ₃	16.64	16.67	16.89	15.91

^a Longest wavelength UV/vis absorption band obtained by multipeak fitting.

Table 6 Kamlet–Taft's α , β , and π^* values of oxide surfaces used in this work, determined by means of dyes 1–3 and eqn (2)–(4)

Sample	α (1)	β (2)	π^* (3)
Silica gel 60	1.14	0.00	0.81
Siral 1.5	1.34	0.43	1.01
Siral 15	1.75	0.52	1.09
Siral 30	1.64	0.44	1.06
Siral 60	1.71	0.51	1.12
Siral 80	1.62	0.31	1.11
MgO	0.67	0.26	0.87
CaCO ₃	0.78	0.29	0.97
ZnO	1.56	0.00	0.71
TiO ₂ (anatase)	1.41	^a	0.85
TiO ₂ (rutile)	1.48	^a	0.86
Al ₂ O ₃	1.32	−0.10	0.94
WO ₃	1.62	^a	1.03
Fe ₂ O ₃	^a	^a	1.21

^a The dye is not recommended for the determination of the parameter, because of photocatalytic decomposition (titanium dioxides), and strong UV/vis self-absorption of tungsten(vi) oxide and iron(III) oxide.

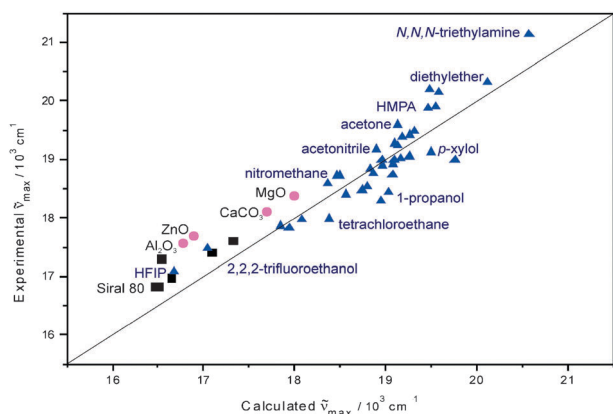


Fig. 12 Correlation of experimental found and calculated wavenumbers of dye 4 dissolved in 38 different solvents (\blacktriangle) and adsorbed onto ten oxidic surfaces (\blacksquare) (longest wavelength UV/vis maximum after multi-peak fitting (\bullet)), obtained using eqn (5a) and the polarity parameters of Table 6 and Table S4 (ESI[†]), respectively.

Consequently, coloured oxides including tungsten(vi) oxide and iron(III) oxide as well as photocatalytic active titanium dioxides (anatase and rutile) were investigated. For these oxidic surfaces not all necessary polarity parameters are available based on the well-established probe dyes 1–3, e.g. due to photocatalytic decomposition of dye 2 (titanium dioxides), and strong UV/vis self-absorption of tungsten(vi) and iron(III) oxide, respectively (see ESI[†]). Compounds 4–7 were adsorbed onto these solids. For tungsten(vi) oxide and titanium dioxides (anatase and rutile) multi-peak fitting was essential because of the complex shape of the UV/vis absorption bands of 4–7 adsorbed onto these surfaces. The β values of tungsten(vi) oxide and rutile were calculated using eqn (5e)–(5m) (Table 3), the longest wavelength UV/vis absorption bands, and the polarity parameters α and π^* from Table 5. For tungsten(vi) oxide a β value of 0 and for rutile a β value of 0.4 were obtained. In the case of anatase, photocatalytic decomposition of the considered dyes was anticipated. The α value for iron(III) oxide of 1.4 was calculated using eqn (5c) and a β value of 0.4 was obtained using

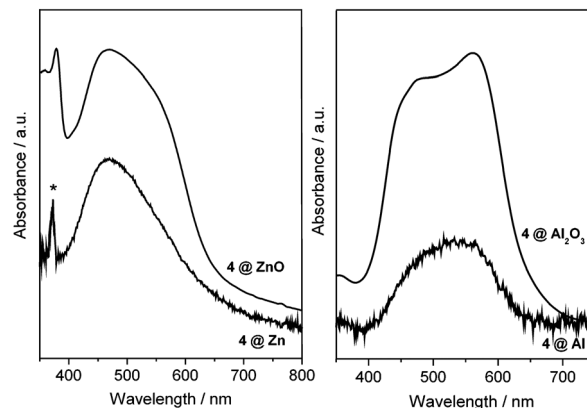


Fig. 13 UV/vis absorption spectra of 4 adsorbed onto zinc/zinc oxide and aluminium/aluminium oxide powders. *Traces of ZnO at the Zn surface.

eqn (5a)–(5c) (Table 3). Therefore, even the polarity parameters of sophisticated surfaces could be obtained using dyes 4–7 in combination with one or two established probe dyes.

Adsorption onto metal surfaces. The interactions of 4 and 7 with surfaces of industrially important metal powders such as iron, copper, nickel, zinc, aluminium, and steel (X65Cr13, 316 L) were probed. Verification of adsorption was achieved by comparison of the intensities of the UV/vis absorption band of the dye solution before and after the adsorption process. In all cases, particularly with semi-noble metals like copper, only a small decrease of the extinction was observed, indicating a low adsorption tendency of 4 and 7 onto these surfaces. Note that the dried, dye-modified metal powders were measured in reflection techniques with a special UV/vis reflectance device and the pristine metal powder as reference sample. However, useful UV/vis absorption spectra were obtained only for zinc and aluminium powders (Fig. 13).

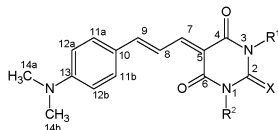
The UV/vis adsorption spectra of 4 adsorbed onto both zinc and zinc oxide as well as onto the aluminium and aluminium oxide surface exhibit the same shape and identical UV/vis absorption maxima. Therefore, solely interactions between 4 and the oxidic centres of the metal powders were measurable. Obviously, valuable UV/vis absorption spectra of dyes 1–3 adsorbed onto the considered surfaces are not available, rendering an adequate determination of the polarity parameters of these surfaces rather difficult.

Experimental

General

Solvents were dried and freshly distilled before use. *N*-Methyl urea (Acros, 97%), malonic acid (ABCR, 99%), trifluoroacetic acid (Riedel-de Haën, +99%), trichloroacetic acid (Riedel-de Haën, 99%), piperidine (Alfa Aesar, 99%), TBAF (1 mol L^{−1} in tetrahydrofuran, ABCR), 1,1,1,3,3,3-hexafluoroisopropanol (fluorochem, 99%), 2,2,2-trifluoroethanol (Acros, 99.8%) were used without further purification. Metals and metal oxides were used as received (BET, purity and source are provided as ESI[†]).

The synthesis and purification of *N*-methylbarbituric acid and dyes **1–7** have been described previously.^{34d,47,65–67}



4, dark violet solid, **yield**: 92% (80%);⁴⁷ **elementary analysis**: $C_{15}H_{15}N_3O_3$ (285.298 g mol⁻¹): found (calc.) [%]: C: 62.99 (63.15), N: 14.85 (14.73), H: 5.14 (5.30); **¹H NMR** (DMSO-*d*₆), δ [ppm]: 3.06 (s, 6H, N-CH₃ (aniline)), 6.80 (d, 2H, 12, $J_{12,11}$ 8.63), 7.55 (d, 2H, 11, $J_{11,12}$ 8.66), 7.62 (d, 1H, 9, $J_{9,8}$ 14.92), 7.97 (d, 1H, 7, $J_{7,8}$ 12.92), 8.22 (dd, 1H, 8), 10.98 (s, br, 1H, NH), 11.04 (s, br, 1H, NH); **¹³C NMR** (DMSO-*d*₆), δ [ppm]: 39.8 (N-CH₃ (aniline))* , 110.4 (5), 112.2 (12), 119.1 (8), 122.8 (10), 131.6 (11), 150.5 (2), 152.9 (13), 155.6 (7), 156.1 (9), 163.5/163.7 (4/6). Crystals of compound **4** for single-crystal X-ray structure analysis were obtained by slow diffusion of water into a dimethylsulfoxide solution of **4**.

5, dark violet solid, **yield**: 83%; **elementary analysis**: $C_{16}H_{17}N_3O_3$ (299.325 g mol⁻¹): found (calc.) [%]: C: 63.98 (64.20), N: 14.01 (14.04), H: 5.57 (5.73); diastereomeric mixture, **¹H NMR** (DMSO-*d*₆), δ [ppm]: 3.06 (s, 6H, N-CH₃ (aniline)), 3.16 (s, 3H, N-CH₃ (barbituric acid)), 6.80 (d, 2H, 12, $J_{12,11}$ 8.91), 7.56 (d, 2H, 11, $J_{11,12}$ 8.94), 7.57 (d, 2H, 11, $J_{11,12}$ 8.94), 7.65 (d, 1H, 9, $J_{9,8}$ 14.89), 8.00 (d, 1H, 7, $J_{7,8}$ 12.35), 8.02 (d, 1H, 7, $J_{7,8}$ 12.35), 8.25 (dd, 1H, 8), 8.26 (dd, 1H, 8), 11.19 (s, br, 1H, NH), 11.24 (s, br, 1H, NH); **¹³C NMR** (DMSO-*d*₆), δ [ppm]: 26.7/27.3 (N-CH₃, (barbituric acid)), 39.3 (N-CH₃ (aniline))* , 110.2/110.3 (5), 112.2 (12), 119.0/119.2 (8), 122.7/122.8 (10), 131.6/131.7 (11), 150.8/150.9 (2), 152.9/152.9 (13), 155.7/156.2 (7), 156.3/156.5 (9), 162.3/162.4/162.8/163.3 (4/6).

6, dark violet solid, **yield**: 75%; **elementary analysis**: $C_{17}H_{19}N_3O_3$ (313.351 g mol⁻¹): found (calc.) [%]: C: 64.94 (65.16), N: 13.46 (13.41), H: 5.92 (6.11); **¹H NMR** (DMSO-*d*₆), δ [ppm]: 3.07 (s, 6H, N-CH₃ (aniline)), 3.20 (s, 6H, N-CH₃ (barbituric acid)), 6.81 (d, 2H, 12, $J_{12,11}$ 9.0), 7.58 (d, 2H, 11, $J_{11,12}$ 8.9), 7.69 (d, 1H, 9, $J_{9,8}$ 14.8), 8.06 (d, 1H, 7, $J_{8,7}$ 2.5), 8.28 (dd, 1H, 8); **¹³C NMR**, (DMSO-*d*₆), δ [ppm]: 27.4 (N-CH₃, (barbituric acid)), 39.2 (N-CH₃ (aniline))* , 111.8 (12), 119.1 (8), 123.0 (10), 131.4 (11), 151.2 (2), 152.8 (13), 156.0 (7), 156.4 (9), 161.5/162.1 (4/6).

7, dark blue-violet solid, **yield**: 79% (91%);⁴⁷ **elementary analysis**: $C_{15}H_{15}N_3O_2S$ (301.365 g mol⁻¹): found (calc.) [%]: C: 59.09 (59.78), N: 13.67 (13.94), H: 4.91 (5.02), S: 10.48 (10.64); **¹H NMR** (DMSO-*d*₆), δ [ppm]: 3.09 (s, 6H, N-CH₃ (aniline)), 6.82 (d, 2H, 12, $J_{12,11}$ 9.37), 7.58 (d, 2H, 11, $J_{11,12}$ 8.98), 7.73 (d, 1H, 9, $J_{9,8}$ 14.45), 8.00 (d, 1H, 7, $J_{7,8}$ 12.50), 8.25 (dd, 1H, 8), 12.09 (s, br, 1H, NH), 12.13 (s, br, 1H, NH); **¹³C NMR** (DMSO-*d*₆), δ [ppm]: 39.5 (N-CH₃ (aniline))* , 110.0 (5), 112.0 (12), 119.2 (8), 122.6 (10), 131.9 (11), 153.2 (13), 156.2 (7), 157.7 (9), 161.1/161.8 (4/6), 177.9 (2).

*The N-CH₃ (aniline) signal was localised by HMQC experiments, because it was covered with the DMSO signal in the ¹³C NMR spectra.

Instrumentation

For the *UV/vis* measurements, a diode array spectrometer MCS 400 from Carl Zeiss Jena GmbH (Jena, Germany) with glass

fibre optics was used. Solutions were measured in transmission with precision quartz cells and an immersion cuvette TSM 5A (Zeiss) while powder spectra were received in reflection with a special reflectance device with unmodified powders as a reference. Spectral analysis was performed with Win-Aspect (version 1.3.1). For multiple regression analysis the Origin Pro (version 8.1) statistic program from OriginLab Corporation was used. Multi-peak fitting was done with IGOR Pro (version 6.2.0.0).

The determination of the *pK_a* values of dyes **4–7** was done in mixtures of ethanol and water (volume ratio 4:3) by titration with 4.6 mol L⁻¹ HCl-solution. The *UV/vis* spectra were recorded with an immersion cuvette TSM 5A (Zeiss). Simultaneously the pH-value was determined with the pH-measuring electrode (Vario pH from WTW, GmbH & Co KG Weilheim, Germany) (accuracy of measurement: ± 0.01 pH). The determination of *pK_a*-values was done by means of the Henderson–Hasselbalch equation.⁶⁸

Sample preparations for *perichromic measurements* were done according to the following procedure. Dyes **1, 4–7** were dissolved in dichloromethane; dyes **2** and **3** were dissolved in cyclohexane. 5 mL of the dye solution per 0.1 g of the metal/metal oxide powder was used. The suspensions were shaken for ten minutes under exclusion of light, decanted and dried under vacuum.

ATR-FT-IR spectra were obtained with a Golden Gate ATR accessory (LOT-Oriel GmbH & Co. KG, Darmstadt, Germany) using a BioRad FT-IR 165 spectrometer (Bio-Rad Laboratories, Philadelphia, PA, USA).

Liquid-NMR-measurements were performed with a Varian UNITY INOVA 400 and a Bruker Avance 250 NMR spectrometer with a ¹H-resonance of 400 MHz and 250.13 MHz, respectively, and a ¹³C-resonance of 100 MHz and 62.90 MHz, respectively. The solvent residue signals were used as internal standards. Coupling constants are given in Hz.

Solid state NMR measurements. ¹³C-¹H}-CPMAS NMR spectra were collected at either 9.4 T (Bruker Avance 400) or 16.4 T (Bruker Avance 700) spectrometers, equipped with commercially available double-resonance probes capable of MAS (magic angle spinning). The spectra were measured either at 100.6 MHz in a 4 mm standard zirconium oxide rotor (Bruker) spinning at 12 kHz or 176.1 MHz in a 1.3 mm zirconium oxide rotor (Bruker) spinning at 40 kHz. Cross polarization with contact times of 3–5 ms was applied to enhance the sensitivity, where the recycle delay was set to 32 s. All ¹³C NMR spectra were collected with TPPM proton decoupling.

¹H MAS NMR data were recorded on a 700 MHz Bruker Avance spectrometer. The experiments were carried out using either 2.5 mm rotors at MAS spinning frequencies of 30 kHz or 1.3 mm rotors at MAS spinning frequencies of 50 kHz and recycle delays of 5–64 s. The back-to-back recoupling sequence was used to excite and reconvert double-quantum coherences,⁶⁹ applying the States-TPPI method⁷⁰ for phase-sensitive detection. Further details are given in the figure captions of the respective 2D spectra. All experiments were performed at room temperature. The spectra were referenced externally with respect to tetramethyl silane using tetrakis(trimethylsilyl)silane as secondary (solid) standard (¹³C: 3.55 ppm, ¹H: 0.27 ppm).

Single-crystal X-ray structure analysis of **4** was performed with an Oxford Gemini S diffractometer at 105 K equipped

with a graphite monochromator, utilising Cu K α radiation ($\lambda = 1.54184 \text{ \AA}$). The structure was solved by direct methods and refined by full matrix least-square procedures on F² using the SHELX⁷¹ software package. All non-hydrogen atoms were refined in the anisotropic approximation against F of all observed reflections. All hydrogen atoms were added on calculated positions, except for NH protons which were found in difference Fourier synthesis. The figures were created using the ORTEP-III und POV Ray program package.

Crystal parameters of **4** are reported as follows: dark violet, C₁₅H₁₅N₃O₃, $M = 285.30 \text{ g mol}^{-1}$; monoclinic, $P2_1/n$, $a = 4.5663(2) \text{ \AA}$, $b = 9.6254(5) \text{ \AA}$, $c = 30.3857(14) \text{ \AA}$, $\beta = 91.668(5)^\circ$, $V = 1334.96(11) \text{ \AA}^3$, $Z = 4$, $D_C = 1.420 \text{ g cm}^{-3}$, 8822 reflections collected in the 4.82–65.53 ω -range, 2277 unique. The final R was 0.1530 for all data.

Elemental analyses were obtained on a Vario EL supplied from Elementaranalysengeräte GmbH (Hanau, Germany).

Conclusions

The solid state packing and the formation of self-complementary aggregates within the structure of dyes **4**, **5** and **7** are governed by intermolecular hydrogen bonds between carbonyl oxygens and NH protons of the barbituric acid moiety as well as the methyl groups of the *N,N*-dimethylaniline ring, as evidenced by solid state NMR and X-ray analysis. (Thio)barbituric acid derivatives **4–7** have a moderate to high solvatochromic range, and high extinction coefficients in different organic solvents. The solvatochromic behaviour of these compounds is dominated by both the dipolarity/polarisability properties and hydrogen bond donating ability of the considered medium. In strong acidic media, protonation of the compounds was observed resulting in a strong hypsochromic shift of the UV/vis absorption band of **4–7**. In strong basic media, the NH-bearing (thio)barbituric acid derivatives **4**, **5**, and **7** show solvatochromic interactions, deprotonation and degradation. In addition, the dimethyl-functionalised barbituric acid derivative **6** is less stable in basic media and solely degradation reactions were observed. Adsorbed onto metal surfaces, interactions between the dyes and oxidic layers were detected, while complex UV/vis adsorption spectra were obtained upon adsorption onto oxidic surfaces. In comparison with the well-established solvatochromic probe dyes **1–3**, the (thio)barbituric acid derivatives **4–7** comprise rather promising candidates for probing surface polarity parameters of coloured oxidic materials.

Acknowledgements

Financial support by the Deutsche Forschungsgemeinschaft and the Fonds der Chemischen Industrie is gratefully acknowledged. We thank P. Kempe for the determination of the BET values.

References and notes

- G. A. Olah, in *Acidity and Basicity, Theory, Assessment and Utility*, ed. J. Fraissard and L. Petrakis, Nato Advanced Study Institute Series C444, Kluwer Academic, Dordrecht, 1994, p. 305.
- (a) R. S. Drago, S. C. Petronius and C. W. Chronister, *Inorg. Chem.*, 1994, **33**, 367; (b) R. S. Drago, J. A. Dias and T. O. Maier, *J. Am. Chem. Soc.*, 1997, **119**, 4444; (c) R. S. Drago, S. C. Dias, M. Torrealba and I. de Lima, *J. Am. Chem. Soc.*, 1997, **119**, 7702.
- (a) A. Corma, *Chem. Rev.*, 1995, **95**, 559; (b) A. Corma, *Curr. Opin. Solid State Mater. Sci.*, 1997, **2**, 63.
- (a) J. B. Jensen, J. B. Nicholas, T. Xu, L. W. Beck and D. B. Ferguson, *Acc. Chem. Res.*, 1996, **29**, 259; (b) T. Xu, N. Kob, R. S. Drago, J. B. Nicholas and J. F. Haw, *J. Am. Chem. Soc.*, 1997, **119**, 12231; (c) J. F. Haw, T. Xu, J. B. Nicholas and P. W. Goguen, *Nature*, 1997, **389**, 832.
- P. Umanski, J. Engelhardt and W. K. Hall, *J. Catal.*, 1991, **127**, 128.
- D. Fargasiu, A. Ghenciu and J. Q. Li, *J. Catal.*, 1996, **158**, 116.
- (a) S. Spange, A. Reuter and D. Lubda, *Langmuir*, 1999, **15**, 2103; (b) S. Spange, S. Prause, E. Vilsmeier and W. R. Thiel, *J. Phys. Chem. B*, 2005, **109**, 7280; (c) S. Spange, D. Kunzmann, R. Sens, I. Roth, A. Seifert and W. Thiel, *Chem.-Eur. J.*, 2003, **9**, 4161; (d) S. Prause, S. Spange and H. Barthel, *Macromol. Chem. Phys.*, 2005, **206**, 364; (e) S. Spange, E. Vilsmeier, K. Fischer, A. Reuter, S. Prause, Y. Zimmermann and C. Schmidt, *Macromol. Rapid Commun.*, 2000, **21**, 643; (f) Y. Zimmermann, S. Anders, K. Hofmann and S. Spange, *Langmuir*, 2002, **18**, 9578; (g) S. Spange, A. Reuter and W. Linert, *Langmuir*, 1998, **14**, 3479; (h) S. Spange, E. Vilsmeier and Y. Zimmermann, *J. Phys. Chem. B*, 2000, **104**, 6417; (i) Y. Zimmermann and S. Spange, *J. Phys. Chem. B*, 2002, **106**, 12524; (j) M. El-Sayed, A. Seifert and S. Spange, *J. Sol-Gel Sci. Technol.*, 2005, **34**, 77; (k) S. Adolph, S. Spange and Y. Zimmermann, *J. Phys. Chem. B*, 2000, **104**, 6429; (l) S. Spange, Y. Zimmermann and A. Graeser, *Chem. Mater.*, 1999, **11**, 3245; (m) S. Prause and S. Spange, *J. Phys. Chem. B*, 2004, **108**, 5734; (n) V. Dutschk, S. Prause and S. Spange, *J. Adhes. Sci. Technol.*, 2002, **16**, 1749.
- (a) C. Rottman, G. S. Grader and D. Avnir, *Chem. Mater.*, 2001, **13**, 3631; (b) C. Rottman, G. S. Grader and D. Avnir, *Langmuir*, 1996, **12**, 5505.
- J. J. Michels and J. G. Dorsey, *Langmuir*, 1990, **6**, 414.
- D. J. Macquarrie, S. J. Tavener, C. W. Gray, P. A. Heath, J. S. Rafelt, S. I. Saulzet, J. J. E. Hardy, J. H. Clark, P. Sutra, D. Brunel, F. di Renzo and F. Fajula, *New J. Chem.*, 1999, **23**, 725.
- Y. Imai and Y. Chujo, *Macromolecules*, 2000, **33**, 3059.
- O. A. El Seoud, A. D. Ramadan and B. M. Sato, *J. Phys. Chem. C*, 2010, **114**, 10436.
- D. Villemin and M. Hachemi, *React. Kinet. Catal. Lett.*, 1994, **53**, 147.
- C. Reichardt and T. Welton, *Solvents and Solvent Effects in Organic Chemistry*, Wiley-VCH, Weinheim, 2011, p. 82.
- E. M. Kosower, *J. Am. Chem. Soc.*, 1958, **80**, 3253.
- V. Gutmann, *Electrochim. Acta*, 1976, **21**, 661.
- C. Reichardt, *Chem. Rev.*, 1994, **94**, 2319.
- M. J. Kamlet, J.-L. M. Abboud, M. H. Abraham and R. W. Taft, *J. Org. Chem.*, 1983, **48**, 2877.
- (a) J. Catalán and C. Diaz, *Eur. J. Org. Chem.*, 1999, 885; (b) P. S. Sierra, C. C. Tejuca, J. Catalán, C. Diaz, F. Garcia-Blanco and G. E. Gorostidi, *Helv. Chim. Acta*, 2005, **88**, 312; (c) J. Catalán, J. Palomar, C. Diaz and J. L. G. de Paz, *J. Phys. Chem. A*, 1997, **101**, 5183; (d) J. Catalán, *J. Org. Chem.*, 1997, **62**, 8231; (e) J. Catalán and H. Hopf, *Eur. J. Org. Chem.*, 2004, 4694; (f) J. Catalán, *J. Phys. Chem. B*, 2009, **113**, 5951.
- IUPAC. *Compendium of Chemical Terminology, 2nd edn (the "Gold Book")*, Compiled by A. D. McNaught and A. Wilkinson, Blackwell Scientific Publications, Oxford, 1997.
- C. Reichardt, *Pure Appl. Chem.*, 2008, **80**, 1415.
- L. C. Fidale, C. Ißbrücker, P. L. Silva, C. M. Lucheti, Th. Heinze and O. A. El Seoud, *Cellulose*, 2010, **17**, 937.
- (a) K. Fischer and S. Spange, *Macromol. Chem. Phys.*, 2000, **201**, 1922; (b) K. Fischer, T. Heinze and S. Spange, *Macromol. Chem. Phys.*, 2003, **204**, 1315; (c) K. Fischer, S. Prause, S. Spange, F. Cichos and C. Borczkyskowski, *J. Polym. Sci., Part B: Polym. Phys.*, 2003, **41**, 1210; (d) K. Fischer, S. Spange, S. Fischer, C. Bellmann and J. Adams, *Cellulose*, 2002, **9**, 31; (e) S. Spange, K. Fischer, S. Prause and T. Heinze, *Cellulose*, 2003, **10**, 201; (f) L. A. Pothan, Y. Zimmermann, S. Thomas and S. Spange, *J. Polym. Sci., Part B: Polym. Phys.*, 2000, **38**, 2546.
- W. Linert, R. F. Jameson, G. Bauer and A. Taha, *J. Coord. Chem.*, 1997, **42**, 211.
- (a) S. Spange and D. Keutel, *Liebigs Ann. Chem.*, 1992, **1992**, 423; (b) S. Spange, M. Lauterbach, A.-K. Gyra and C. Reichardt, *Liebigs Ann. Chem.*, 1991, **1991**, 323; (c) R. Lungwitz,

- M. Friedrich, W. Linert and S. Spange, *New J. Chem.*, 2008, **32**, 1493; (d) S. Spange, A. Reuter, E. Vilsmeier, T. Heinze, D. Keutel and W. Linert, *J. Polym. Sci., Part A: Polym. Chem.*, 1998, **36**, 1945; (e) S. Spange, F. Simon, G. Heublein, H. J. Jacobasch and M. Boerner, *Colloid Polym. Sci.*, 1991, **269**, 173; (f) S. Spange and G. Heublein, *Z. Chem.*, 1989, **29**, 142; (g) S. Spange, P. Hortschansky and G. Heublein, *Acta Polym.*, 1989, **40**, 602; (h) S. Spange, C. Schmidt and H. R. Kricheldorf, *Langmuir*, 2001, **17**, 856; (i) L. A. Pothan, Y. Zimmermann, S. Thomas and S. Spange, *J. Polym. Sci., Part B: Polym. Phys.*, 2000, **38**, 2546; (j) I. Kahle and S. Spange, *J. Phys. Chem. C*, 2010, **114**, 15448.
- 26 M. Podsiadla, J. Rzeszotarska and M. K. Kalinowski, *Collect. Czech. Chem. Commun.*, 1994, **59**, 1349.
- 27 G. Heublein, U. Erler, A. Ulbricht and H. Winkelmann, *Angew. Makromol. Chem.*, 1990, **182**, 29.
- 28 I. Georgieva, A. J. A. Aquino, N. Trendafilova, P. S. Santos and H. Lischka, *Inorg. Chem.*, 2010, **49**, 1634.
- 29 I.-W. Kim, M. D. Jang, Y. K. Ryu, E. H. Cho, Y. K. Lee and J. H. Park, *Anal. Sci.*, 2002, **18**, 1357.
- 30 A. Taha, A. A. T. Ramadan, M. A. El-Beairy, A. I. Ismail and M. M. Mahmoud, *New J. Chem.*, 2001, **25**, 1306.
- 31 T. Tlaczala and A. Bartecki, *Monatsh. Chem.*, 1997, **128**, 225.
- 32 M. Podsiadla, J. Rzeszotarska and M. K. Kalinowski, *Monatsh. Chem.*, 1994, **125**, 827.
- 33 A. Al-Alousy and J. Burgess, *Inorg. Chim. Acta*, 1990, **169**, 167.
- 34 (a) A. Oehlke, K. Hofmann and S. Spange, *New J. Chem.*, 2006, **30**, 533; (b) R. Lungwitz and S. Spange, *New J. Chem.*, 2008, **32**, 392; (c) S. Spange, D. Kunzmann, R. Sens, I. Roth, A. Seifert and W. Thiel, *Chem.-Eur. J.*, 2003, **9**, 4161; (d) S. Spange, R. Sens, Y. Zimmermann, A. Seifert, I. Roth, S. Anders and K. Hofmann, *New J. Chem.*, 2003, **27**, 520.
- 35 O. A. El Seoud, A. R. Ramadan, B. M. Sato and P. A. R. Pires, *J. Phys. Chem. C*, 2010, **114**, 10436.
- 36 L. A. Pothan and S. Thomas, *Compos. Sci. Technol.*, 2003, **63**, 1231.
- 37 A. A. Gorman, M. G. Hutchings and P. D. Wood, *J. Am. Chem. Soc.*, 1996, **118**, 8497.
- 38 S. Seifert, S. Spange, unpublished results.
- 39 K. Nakashima and S. Akiyama, *Chem. Pharm. Bull.*, 1981, **29**, 1755.
- 40 B. C. Wang and B. M. Craven, *J. Chem. Soc. D*, 1971, 290.
- 41 W. Hänsel and S. Umlauff, *Pharm. Unserer Zeit*, 1993, **22**, 207.
- 42 R. Gup, E. Giziroglu and B. Kirkan, *Dyes Pigm.*, 2007, **73**, 40.
- 43 (a) P. Flores, M. C. Rezende and F. Jara, *Dyes Pigm.*, 2004, **62**, 277; (b) M. C. Rezende, P. Campodonico, E. Abuin and J. Kossanyi, *Spectrochim. Acta, Part A*, 2001, **57**, 1183; (c) F. Jara, C. Mascayano, M. C. Rezende, C. Tirapegui and A. Urzua, *J. Inclusion Phenom. Macrocyclic Chem.*, 2006, **54**, 95; (d) C. Tirapegui, F. Jara, J. Guerrero and M. C. Rezende, *J. Phys. Org. Chem.*, 2006, **19**, 786.
- 44 A. V. Kulinich, N. A. Derevyanko and A. A. Ishchenko, *Russ. J. Gen. Chem.*, 2006, **76**, 1441.
- 45 M. Bauer, A. Rollberg, A. Barth and S. Spange, *Eur. J. Org. Chem.*, 2008, 4475.
- 46 (a) B. S. Jursic, *J. Heterocycl. Chem.*, 2001, **38**, 655; (b) B. S. Jursic and E. D. Stevens, *Tetrahedron Lett.*, 2003, **44**, 2203.
- 47 M. Strell and S. Reindl, *Arch. Pharm.*, 1960, **293**, 984.
- 48 S. Akiyama, K. Nakashima, S. Nakatsuji, M. Suzuki and C. Umekawa, *Dyes Pigm.*, 1987, **8**, 459.
- 49 M. K. Haldar, M. D. Scott, N. Sule, D. K. Srivastava and S. Mallik, *Bioorg. Med. Chem. Lett.*, 2008, **18**, 2373.
- 50 See selected publications: Y. Kawabe, H. Ikeda, T. Sakai and K. Kawasaki, *J. Mater. Chem.*, 1992, **2**, 1025.
- 51 F. G. Webster, W. C. McColgin and Fr. Demande, *FR 2156723 19730706*, 1973.
- 52 A. F. Vompe, G. F. Kuepina, A. V. Borin, N. S. Vulfson, A. G. Vakar, M. A. Guskova, G. E. Vasilenko, L. V. Ivanova, S. I. Ryskina and N. V. Siletskaya, *SU 163071 19640527*, 1964.
- 53 T. Kripp, T. Czigler and P. A. Semadeni, *PCT Int. Appl.*, 2000, **WO 2000052100**.
- 54 M. Ikeda, K. Shigaki and T. Inoue, *PCT Int. Appl.*, 2002, **WO 2002071530 A1 20020912**.
- 55 R. Lu, S. G. Chen, X. D. Cao, W. S. Yang, Y. Y. Jiang and T. J. Li, *Synth. Met.*, 1995, **71**, 2035.
- 56 (a) M. Khan, V. Enkelmann and G. Brunklaus, *J. Am. Chem. Soc.*, 2010, **132**, 5254; (b) I. Bolz, C. Moon, V. Enkelmann, G. Brunklaus and S. Spange, *J. Org. Chem.*, 2008, **73**, 4783.
- 57 W. Bolton, *Acta Crystallogr.*, 1963, **16**, 166.
- 58 M. Khan, V. Enkelmann and G. Brunklaus, *J. Org. Chem.*, 2009, **74**, 2261.
- 59 (a) B. Elena, G. Pintacuda, N. Mifsud and L. Emsley, *J. Am. Chem. Soc.*, 2006, **128**, 9555; (b) C. J. Pickard, E. Salager, G. Pintacuda, B. Elena and L. Emsley, *J. Am. Chem. Soc.*, 2007, **129**, 8932; (c) F. Taulelle, *Solid State Sci.*, 2004, **6**, 1053; (d) J. Senker, L. Seyfarth and J. Voll, *Solid State Sci.*, 2004, **6**, 1039; (e) M. Khan, V. Enkelmann and G. Brunklaus, *CrystEngComm*, 2011, **13**, 3213.
- 60 R. K. Harris, Y. Phuonng, B. Robert, C. Y. Ma and K. J. Roberts, *Chem. Commun.*, 2003, 2834.
- 61 T. Emmmler, S. Gieschler, H. H. Limbach and G. Buntkowsky, *J. Mol. Struct.*, 2004, **700**, 29.
- 62 T. Gorelik, G. Matveeva, U. Kolb, T. Schleuß, A. F. M. Kilbinger, J. van de Streek, A. Bohle and G. Brunklaus, *CrystEngComm*, 2010, **12**, 1824.
- 63 J. P. Bradley, C. Tripon, C. Filip and S. P. Brown, *Phys. Chem. Chem. Phys.*, 2009, **11**, 6941.
- 64 Y. Marcus, *Chem. Soc. Rev.*, 1993, **22**, 409.
- 65 I. Devi and P. J. Bhuyan, *Tetrahedron Lett.*, 2005, **46**, 5727.
- 66 A. A. Schilt, *J. Am. Chem. Soc.*, 1960, **82**, 3000.
- 67 R. W. Kenyon, D. F. Newton and D. Thorp, *Chem. Abstr.*, 1993, **113**, 134174v.
- 68 K. A. Connors, *Binding Constants*, J. Wiley & Sons, New York, 1987.
- 69 (a) W. Sommer, J. Gottwald, D. E. Demco and H. W. Spiess, *J. Magn. Reson.*, 1995, **A113**, 131; (b) M. Feike, D. E. Demco, R. Graf, J. Gottwald, S. Hafner and H. W. Spiess, *J. Magn. Reson.*, 1996, **A112**, 214; (c) K. Saalwächter, R. Graf and H. W. Spiess, *J. Magn. Reson.*, 1999, **140**, 471; (d) K. Saalwächter, R. Graf and H. W. Spiess, *J. Magn. Reson.*, 2001, **148**, 398.
- 70 D. Marion, M. Ikura, R. Tschudin and A. Bax, *J. Magn. Reson.*, 1989, **85**, 393.
- 71 (a) G. M. Sheldrick, *SHELXL-97*, Program for Crystal Structure Refinement, 1997; (b) G. M. Sheldrick, *Acta Crystallogr., Sect. A: Found. Crystallogr.*, 1990, **46**, 467.